GPS Measured Response of a Tall Building due to a Distant Mw 7.3 Earthquake

GPS measured response of a tall building due to a distant Mw 7.3 earthquake

Thomas Herring[1], Chen Gu[1], M. Nafi Toksöz[1], Jafarali Parol[2], Abdullah Al-Enezi[2], Farah Al-Jeri[2], Jamal Al-Qazweeni[2], Hasan Kamal[2], Oral Büyüköztürk[1]

[1]Massachusetts Institute of Technology, 77 Massachusetts Avenue, Cambridge, MA 02139 USA

[2]Kuwait Institute for Scientific Research, Kuwait City, 13109, Kuwait

ABSTRACT *(250 word limit)*

The response of a 413-meter-tall building to the 12 November, 2017, Mw 7.3 earthquake 642-km from the building is measured with a GPS receiver located near the top of the building and operating with a 1 Hz sampling rate. Nearby GPS and seismic stations measure the ground motion near the building. The ground motions have amplitudes of ~40 mm while the top of the building moves by up to 160 mm. The building motion continues with levels greater than the noise level of the GPS measurement for about 15 minutes after the earthquake. After the ground motion excitation ends, the building motion decays with a time constant of ~2 minutes and the beat between the two lowest frequency modes of deformation of the building can be seen. There are two large amplitude peaks in the building motion with magnitudes of 120 and 160 mm. The timing of the peaks is consistent with ground excitation in a 8.3-6.5 second period (120-180 mHz) band which covers the 7.25 and 5.81 second periods (138 and 172 mHz frequencies) of the fundamental modes of the building. The ground motions in this band show two large pulses of the excitation which have timing consistent with the large amplitude building signals. The response of the top of the building is amplified by an order magnitude over the ground motions in this band. There is no apparent permanent displacement of the top of the tower.

Keywords Building Earthquake response, seismic surface waves, building fundamental mode excitation, GPS measurements.

Short Title: GPS measured response of a tall building due to a distant earthquake (70-characters max)

INTRODUCTION

There is an increasing number of tall and ultra-high buildings in the world, including the Arabian Peninsula. These tall buildings are greatly affected by long trains of seismic waves from regional earthquakes with the seismic motions being greatly amplified with the increasing height of the buildings (Shakal et al., 1996; Çelebi and Liu, 1998; Çelebi et al., 2014). In this paper, we show the GPS measured response of the tallest building in Kuwait, the Al-Hamra Tower, to the 12 Nov 2017 Mw 7.3 earthquake, 642 km to the north, on the Iran-Iraq border.

The Al-Hamra Tower is a unique, sculpted building, 413 m tall with 86 floors (Figure 1). It is a steel, reinforced concrete structure. The foundation of the tower is supported by 289 reinforced concrete piles, ranging in depth from 22 m to 27 m. There is an extended apron shopping mall which is isolated from the tower. The Tower's response to ground vibrations has been calculated using detailed structural design information and finite element modeling (Al-Qazweeni et al., 2018, Sun and Büyüköztürk, 2018). The building vibration has been measured, with temporary occupations, using one Kinemetrics EpiSensor instrument at the 80th floor of the Al-Hamra Tower. Many studies have used ambient vibrations to determine the response of buildings (Kohler et al., 2005; Snieder and Şafak, 2006; Prieto et al., 2010; Sun et al., 2017; Mordret et al., 2017). Deformations of the building due to annual and daily temperature variations have been determined by GPS measurements on the 86th and 80th floors of the building (Coccia, 2017; Herring et al., 2018).

The vibrational modes of the Al-Hamra Tower have been determined by ambient noise monitoring at the 80th floor of the building and GPS measurements at the 86th floor. The most prominent modes are North/South with a period of 7.1 sec, East/West 5.7 sec period and a torsional model with 3.1 sec period (Toksöz et al., 2018). Similar mode periods are obtained from both ambient noise monitoring on the 80th floor and GPS measurements on the 86th floor.

The 12 Nov 2017 Mw 7.3 earthquake, with epicenter at the Iran-Iraq border (34.905° N, 45.956° E and 19.0km from IRIS), 642 km NNE of Kuwait City, was widely felt in Kuwait. This earthquake is a thrust event with fault plane: Strike = 351°, Dip = 16° and Rake = 137° (U.S. Gelogical Survey [USGS], 2017). The Mw 7.3 earthquake was recorded by both the GPS and seismic stations in Kuwait (Figure 2) and is the first distant earthquake recorded by the GPS building monitoring system. The east component displacement at the top of the Al-Hamra Tower (~ 16 cm) and at the ground level (~ 4 cm) shows the amplification effects of 4 to 5 times. These successful GPS measurements of building response shows GPS to be a useful method to evaluate amplification effects of tall buildings due to seismic ground shaking.

DATA AND METHOD

Seismic Sites and Data Analysis

The Mw 7.3 earthquake was recorded by the Kuwait National Seismic Network (KNSN) operated by the Kuwait Institute for Scientific Research (KISR) (Gu et al., 2018). The KNSN consists of six broadband stations (KB, MI, QR, RD, RS and UM) and two short-period stations (AB and SA) (Gu et al., 2017). The locations of the eight stations are shown in Figure 2b. Stations KB, QR, RS, UM, AB and SA were operational at the time of the Mw 7.3 earthquake with KB being the nearest station to the Al-Hamra Tower. We calculated ground displacements at the KB site (Figure 2c). The broadband seismometers used in this study measure ground velocity in digital counts which are converted to physical units of mm/s through the known response function of the instrument. The displacements are computed by integration of the velocities in the frequency domain which allows the effects of high and low frequency noises to be minimized in the integration. In detail, we first removed the instrument response from the raw ground velocity by deconvolving the instrument response function and converted the raw ground velocity in units from COUNTS to nm/s, using the TRANSFER function of the Seismic Analysis Code (SAC) software (Helffrich et. al., 2013). A quarter-cycle cosine taper, with unit response between 0.0125 Hz (80 sec) and 8.0 Hz (0.125 sec) and zero below 0.01 Hz (100 sec) and above 10.0 Hz (0.1 sec) , was applied during the deconvolution to dampen the response at very low and high frequencies. The instrument response files were created at KISR using the Seisan earthquake analysis software (Havskov and Ottemoller, 1999). We then converted the ground velocity to ground displacement. The conversion was implemented by transforming the time-series velocity seismograms to the frequency domain, converting velocity spectra to displacement spectra in the frequency domain and transforming the resultant displacement spectra to time domain.

GPS Sites and Data Analysis

The Al-Hamra building poses challenges for mounting a GPS antenna primarily due to irregular shape of the top of the building. This is the world's tallest sculptured building consisting of a concrete core with an iconic curtain wall wrapped around the core. The building's concrete core is stone clad outside the curtain wall, and the curtain wall wraps to cover all of the concrete core except for the south facing façade. The building was designed by Skidmore, Owings and Merrill LLP, Chicago (SOM) (https://www.som.com/projects/al_hamra_tower). In order to mount the GPS antenna as high as possible, the GPS antenna is installed near the top of the curtain wall in an accessible area where the supports for the window washing system attaches to the building. We refer to this site with the 4-character code ALHR. This location in shown in Figure 3 along with an image of the GPS antenna protruding ~0.5 meters above the edge of the curtain wall. There is blockage of the satellite signals in the azimuth range of 240^o-300^o where the minimum angle that satellites can be seen can be limited to 40^o (azimuth ~265^o), i.e. near this azimuth no satellites are seen with elevation angles less than 40^o. This blockage is due to the rising edge of the curtain wall. This edge not only blocks signals but also reflects signals from other directions resulting in phase errors from the sum of the direct and reflected signals. These errors are referred to as multipath. They increase the root-mean-square (RMS) scatter of ionospheric free phase residuals to an average of 12 mm for ALHR compared to 9 mm for a typical GPS site (the GPS site locate at the KISR facility in this case).

There are two GPS sites that are used as reference sites for measuring the motions of the top of the tower. One site is located on the roof of the mall connected to the Al-Hamra Tower (MLRF), and it suffers from an obstructed sky view partly from the tower itself but more critically by high-rise buildings to the east of the site. The MLRF site is only 145 meters horizontally from the roof site and 370 meters below the Al-Hamra Tower site, ALHR. However, the site is south of the tower and due to the common inclination of the GPS satellite orbits (~55^o), the region of the sky in which no GPS satellites ever appear is filled with the tower and consequently the tower is of little impact. The buildings to the east have a direct impact on the quality of the data. We are evaluating the location of the site and the GPS antenna is temporarily mounted on a tripod at this location. There is significant sky blockage at this site from other buildings, and this diminishes its usefulness as a reference site. The approximate location of this site is shown in Figure 2b. The primary reference site for our GPS processing is located on a 2-story building at the Kuwait Institute for Scientific Research. This is permanently mounted to the building and is referred to a KISP (with the P denoting the permanent site). KISP is about 9.4 km from ALHR. Its view of the sky is largely unobstructed and it generate GPS phase data of typical quality.

Multipath effects in GPS have a very general form in that it generates periodic oscillations in the phase residuals as the relative path lengths between the direct and reflected signal change. The general nature of the effects has been well studied including the impact on the signal-to-noise of the phase measurements (see e.g., Bilich and Larson, 2007*)*. There are two characteristics of importance in this paper (1) the period of the phase oscillations and (2) the repeating nature of the GPS ground tracks that results in the multipath phase errors repeating each day but occurring approximately 245 seconds earlier each day (Choi et al., 2004).

The period of oscillation of the multipath error depends on the distance to the reflector from the GPS antenna and the angular rate of motion of the satellite being evaluated. Typically, 8-14 GPS satellites can be seen at any time and the position estimate (in kinematic mode where positions are estimated at every data epoch) will be averaged over the visible satellites. If some of the satellites being observed have strong, oscillatory multipath signals, then the position estimates are also likely to show oscillatory errors. This type of behavior is often seen from strong ground reflections. In the obstructed environment of the ALHR site, it is possible that oscillatory position changes of the type expected for seismic wave arrivals and the natural frequency response of the building might arise from multipath. The details of the multipath response depend on the exact geometry but we can approximately determine the period of oscillations based on simple geometric path differences and the angular rate of motions of GPS satellites. GPS satellites orbit with a ~12-sidereal hour period and this orbital period sets the angular rate of motion of the satellites. Using the standard expressions of the phase error due to multipath (Bilich and Larson, 2007*)*, it is easy to derive the minimum period for the multipath effect of the reflection h_λ from the antenna is 3440/h_λ seconds, where h_λ is the distance in wavelengths (190 and 255 mm for L1 and L2, respectively) i.e., a reflector one wavelength from the antenna would be expected to generate oscillations with a period of an hour or more. In our analysis, we will be interested in signals with periods less than 10 seconds. To generate such high frequency signals, reflectors would need to be ~344 wavelengths or 65 meters from the antenna. Coherent reflectors at this distance at the top of the building are unlikely. There are reflecting surfaces at the ALHR site that are within 10 meters of the antenna and reflections from these surfaces could be expected to generate oscillatory position estimates with periods of about 1 minute. We do see such behavior in the ALHR kinematic position estimates.

The other definitive test for multipath we can use is to examine the behavior of the position estimates the days before and after the day of interest. Since the satellite orbits repeat, multipath signals will repeat each day (shifted by ~245 seconds) and if the same data and parameterization are used each day for the position estimates, the multipath error will map into the position estimates in the same way each day. This repeating pattern is the basis of sidereal filtering of high rate kinematic positioning (Genrich and Bock, 1992, Choi et al., 2004, Agnew and Larson, 2007). We use this approach to evaluate the possible impact of multipath but we do not apply any corrections for multipath using this approach because the effects are small enough not to warrant it. To mitigate the effects of multipath on the position estimates and to better show the seismic signals arrivals, we analyze the residual station position motions after removing a smoothed version of the estimates. For convenience, we use a locally weighted regression, LOESS, algorithm, (Cleveland, and Devlin, 1988) with a 60-second span. The details of this smoother do not affect the interpretation of the seismic arrivals which have much shorter periods. The filter reduces the visual impact of the longer period multipath contributions to the position estimates. Genrich and Bock (2006) and Saunders et al. (2016) have previously noted GPS multipath effects at seismic frequencies are generally small but at longer periods (1 minute and greater) they can be large. At these longer periods, errors in modeling and estimating atmospheric delays can also be large as noted in the above references.

The GPS data analyzed for this paper were collected with a 1-Hz sampling rate with 3 receivers in Kuwait, all within 10 km of each other, and receivers from other locations that are operated as part of the International GNSS Service (IGS) global network (Dow et al., 2009). Table 1 summarizes the locations of the GPS and seismic sites used in this paper. The locations of the earthquake and the GPS and seismic stations are shown in Figure 2 with detailed locations in Figure 2b. For the analyses presented here, we rely mostly on the GPS data from the Kuwait sites, KISP and ALHR, and the Haifa, Israel IGS site, BSHM. The other GPS sites were used to validate the results from the primary GPS sites. The GPS antennas at all of the primary sites were mounted on building rooftops but all these buildings were low (a few stories high) except for the one which is mounted at the 86^{th} floor of the Al-Hamra Tower in Kuwait City (ALHR).

The GPS data from these receivers were analyzed using the MIT GAMIT/GLOBK GPS analysis package (Herring et al., 2017) in kinematic mode. In this style of analysis, one station is held fixed and the positions of the other sites are estimated relative to the fixed station. The positions of the site are estimated at the sampling rate of the GPS carrier phase and pseudorange measurements (1Hz). The GPS data were processed in the linear combination of the L1 (1.575 GHz) and L2 (1.227 GHz) measurements which removes the dispersive effects of the Earth's ionosphere. This combination is referred to as the ionospheric free observable. The orbits of the GPS satellites were fixed at the values given by the IGS final orbit product (Dow et al., 2009). The one hour data (18:00-19:00 GPST) that spans the earthquake were processed for the day before, after, and the day of the earthquake. The data of the non-earthquake days were processed to estimate the noise levels in the position estimates on the day of the earthquake. Errors in the satellite and ground stations clock, which directly map in to the phase and pseudo-range measurements, were not estimated but rather these parameters were eliminated from the observation equations by differencing data between satellites and station. This method of processing is referred to as double differencing. In double differences, the numbers of cycles of phase related to the initial unknown phase of the satellite and station oscillators when a receiver first starts tracking a satellite, should be integer if all the correct calibrations and antenna phase centers are used. These initial phase values are often referred to as ambiguities. The values of the ambiguities are initially estimated as fractional values (i.e., non-integer value). In many cases, the number of integer cycles can be determined from the fractional estimates. These integer values are fixed in the kinematic data processing (see Bock and Melgar (2016) for recent review of GPS processing algorithms and applications). For the processing, here 80-100% of the ambiguities could be fixed to integer values depending on specific stations and the site separations. Fewer ambiguities are fixed in analyses with widely separated sites (1000-2000 km).

In addition to the kinematic site position estimates every second, the values of the number of cycles of phase (expressed as the L1/L2 linear combination) that could not be fixed to integer values and one constant differential atmospheric delay between each station and the reference station were included in the Kalman filter state vector. A smoothing Kalman filter was used resulting in non-integer phase ambiguities being constant for the smoothing loop. The process noise values for the position estimates are large and hence the "smoothing" filter does not smooth the position estimates. It is used so that estimated ambiguities and atmospheric delay estimates are constant.

There is always an issue of possible motions of the reference station for earthquake studies using differential GPS processing. Ideally, the reference station is far enough away from the earthquake or is in a null in the radiation pattern so that it does not have any motion from propagation of seismic waves. The GPS sites in Table 1 outside of Kuwait were chosen to evaluate possible motions of different reference sites. Table 2 gives the distances and azimuths between the earthquake epicenter and various GPS and seismometer sites. The Kuwait reference site (KISP) and the Al-Hamra 86th floor site (ALHR) are about 640 km from the epicenter and their epicentral distances differ by only 1.7 km. This similarity in distance suggests that the ground motion at KISP and ALHR should occur at about the same time and be of similar magnitude if the site conditions are similar at the two locations. The KB seismic station is 12 km further from the epicenter indicating that arrivals there could be 2-3 seconds after arrivals at KISP depending on the wave type. The primary GPS reference site outside of Kuwait that we use is the BSHM site. It is 1038 km from the epicenter, indicating that arrivals there will be later than KISP and should be diminished by the greater distance. Results will be presented using BSHM and KISP GPS sites as base stations. The motions of ALHR relative to BSHM will give the absolute motion of ALHR provided BSHM is not strongly affected by the earthquake, and motions relative to KISP will give the building response provided the ground motion at KISP and Al-Hamra are the same. The GPS data from the Al-Hamra Mall site (MLRF) can validate this latter assumption, but the results from MLRF site are noisier than other sites partly due to the obstruction of the sky view by the Al-Hamra Tower and other high rise buildings (see the supplementary materials)..

GROUND SURFACE AND BUILDING MOTIONS

The 1-Hz GPS data from the local Kuwait and global GPS stations have been analyzed multiple times using different station selections and parameter settings in the GAMIT/GLOBK kinematic Kalman filter program (track). These analyses were aimed at assessing whether significant seismic signal arrivals at the reference station used for kinematic positioning could be detected and whether the response of the Al-Hamra building could be separated from the ground motion at the base of the building. The results presented here are our assessments of these questions.

The nearest IGS GPS site that records 1 Hz data is BSHM and is located in Haifa, Israel. This site is just over 1000 km from the epicenter and surface wave arrivals at about 400 seconds after the event might be expected. To test if these arrivals may have affected the Kuwait results, we processed the Kuwait GPS sites relative to this station and relative to the four other distant sites shown in Table 1. The motions at the Kuwait sites were similar for all these reference sites indicating that seismic induced motions at BSHM are likely to be less than 10 mm. Directly processing the BSHM data relative to KIT3 and NICO and using the same analysis methods as used for the Kuwait sites shows no motions greater than 8 mm in the horizontal components at the time of the expected arrivals. We also obtained broadband seismic data from the seismic station in Malkishua, Israel (MMLI) and integrated these data to displacement (see Data and Resources section). These results show surface wave arrivals between 300 and 400 seconds after the earthquake with amplitudes of ~5mm. These amplitudes are much less than the arrivals at the Kuwait stations.

The three main GPS results are shown in Figures 4-6. The comparison of measured displacements from GPS station KISP w.r.t. BSHM/ALHR w.r.t. BSHM and seismic station KB is shown in Figure 4 and 5. The motions are shown in the north, east and up directions for the 15 minutes following the earthquake with the LOESS robust smoothed signal with a span of 60 seconds removed from the GPS time series. The seismic results have been offset in time by 2.5 seconds to account for the different epicentral distances. In Figure 6a, we also show the ambient noise spectra from one Kinemetrics EpiSensor accelerometer at the 80th floor of the Al-Hamra Tower. Average spectra for 3 July, 2017, were computed with a 600 s moving window. We marked the longest six periods of the building. Figure 6b shows the horizontal motions of ALHR relative to KISP. If the motions at KISP are the same as the ground motions at the Al-Hamra site, then this figure’s motions show the building response to the earthquake ground motions.

Several features are immediately apparent in the figures. The peak ground motions at the KISP GPS site and KB seismic site see a strong Love wave arrival at about 195 seconds after the event and a Rayleigh wave at 270 seconds. The peak amplitudes of these waves are <50 mm. The details of the seismic and GPS position changes differ most likely due to the different locations of the sensors. (The large peak in the north component at the KB site between 230-240 sec is not seen at either of the GPS sites at KISP or MLRF. Both of these locations are much closer to the downtown area of Kuwait city). An S-wave arrival can be seen in the seismic signal at 155 seconds. This arrival is at the noise level in the GPS time series at KISP. The motions at ALHR are much larger as would be expected given the height of the building. The S-wave arrival at 155 seconds is very clear and the peak at this time has amplitudes of ~15 mm with respect to BSHM and a slightly smaller value of ~12 mm relative to KISP. A large amplitude signal at ALHR, ~120 mm, occurs at 210 seconds is due to the response to the Love wave, but the largest amplitude oscillations occur at 353 seconds with amplitudes of ~160 mm (from the vector sum of the east and north displacements) are due to the response of the Airy phase of Rayleigh waves. After these large peaks, there is largely an exponential decay of the signal amplitude with a time constant of ~2 minutes (e-folding time i.e., the length of time needed for the signal to decay to 1/e (~37%) of its original amplitude). There is also a beat signal present during the decay with a period of ~30 seconds. This beat, with its almost total cancellation in the North components, is consistent with equal amplitude signals at the first two bending modes of the building with periods of 7.27 and 5.82 seconds (measured with GPS), and 7.09 and 5.70 seconds (measured with accelerometer). The same beat can be seen in the east component, but in this case the amplitudes of the two modes differ.

The motions in Figures 5 and 6 look very similar but there is one very clear difference in the height component. The Rayleigh wave height component is very clear in Figure 5 but cannot be clearly seen in Figure 6. This behavior is consistent with the Rayleigh wave being similar in amplitude and timing at the KISP and ALHR locations (also suggested by the seismic KB results) and that the building acts passively with respect to these waves as would be expected i.e., the building simply moves up and down with the motion of the ground. Although vertically propagating waves are expected to be excited by the ground motions, the GPS results do not have the sensitivity to see these effects.

There are two large pulses of the amplitudes in the ALHR response with the largest amplitudes occurring ~350 seconds after the earthquake and ~200 seconds after the first response of the building. The peak amplitude ground motion occurs at ~270 seconds after the earthquake and this is 80 seconds before the largest amplitude building motions. The excitation of the building was studied by computing the moving average amplitude of the amplitude computed over a moving 10-sec window to generate a measure of the response of the building. (Increasing this window length smooths the response but does not affect the nature of the response.) The building has two fundamental bending modes with periods of 7.25 and 5.81 seconds (frequencies of 138 and 172 mHz) as measured by GPS. To assess the power of the ground motions in this frequency band, the GPS and seismic ground motions were bandpass filtered between 120 and 180 mHz (period range 8.3-6.5 seconds) and their moving average RMS amplitude over 10-second windows computed. The comparison is shown Figure 7. For clarity in this figure, the amplitude of the ground excitation has been multiplied by a factor of 10. This factor implies the building response is 10 times larger in this frequency band than the ground motions.

DISCUSSION AND CONCLUSIONS

The installation of GPS antennas on and around tall buildings can be difficult due to obstructions and the effects of signal reflections from nearby structures. In the results presented here, obstruction issues arise but still for the GPS antenna mounted near the top of the Al-Hamra Tower they have not prevented the detailed measurements of the response of the building to a distant Mw 7.3 earthquake. We are able to measure the motions of the top of the Al-Hamra building relative to a very distant GPS site (~1300 km away) and nearby GPS sites 9 kilometers and 140 meters away. The nearest GPS site near the base of the tower is noisy due to obstructions from other nearby buildings in downtown Kuwait City. Its motions are similar to the 9 km distant site at the Kuwait Institute for Scientific Research (KISR) and, in this initial analysis, we have taken the motion at KISR to represent the ground motions at the base of the Al-Hamra Tower. We have used GPS data collected the days before and after the earthquake to determine the noise levels in the GPS measurement in the absence of earthquake excitations. For the ALHR 86th floor GPS receiver, the root-mean-square (RMS) scatters of the north, east and height 1-Hz position measurements are 2.1, 2.8, and 4.7 mm, respectively. The earthquake induced motions have amplitudes of up to 160 mm in north and east, and 30 mm in height.

The GPS sites are near the sea located on the so-called coastal flats (Al-Sulaimi and Mukhopadhyay, 2000) while the KB seismic station is located on the sand flats (*ibid*). Both locations are part of the undifferentiated Fars and Ghar formations. Abdel-Fattah et al., (2013) report that the underground soil sediments in most of Kuwait City can be broadly classified into two types based on the shear-wave velocity in the upper 30 m of soil/bedrock materials. The estimated shear wave Vs30 values ranged between 280 m/s and 510 m/s. The precise details of the geology of the region and the properties of shallow geotechnical layer are not that critical to this study. For the long period waves used in this study, where wavelengths are between 3 and 30 km, local variations in shallow (<100 m) geotechnical properties do not have significant effects on ground displacements.

The November 12, 2017 Mw 7.3 earthquake, 642-km from Kuwait on the Iran-Iraq border, induced ground motions of ~40 mm amplitude. The top of the Al-Hamra Tower moved with amplitudes of up to 160 mm and motions detectable with GPS persisted for about 15 minutes after the earthquake and for about 12.5 minutes after the S-wave arrival at the tower.

After excitation from the earthquake subsided about 350 seconds after the event, the building response can be seen to decay with ~2-minute e-folding time. The beat between the building's two fundamental modes, with frequencies of 138 and 172 mHz, was responsible for the increasing and decreasing amplitudes of the measured oscillations.

The response of the building appears to be directly related to the power in the frequency band between the two fundamental modes of the building. Within the band, the building motions are amplified by about an order of magnitude. There are two main pulses of energy in this band and the building responds with two episodes of shaking. For building occupants, the motions could be disturbing because the initial oscillations with an amplitude of ~100 mm decays over a minute or so but are then is followed about 2 minutes later by larger 150 mm amplitude oscillations. The period of the oscillations is about 6.5 seconds and there is a beat envelope with a period of ~30 seconds. During the decay of the oscillations, the amplitudes of the two fundamental modes in the north direction are very similar and their beat decays almost to zero amplitude each cycle.

After about 15 minutes the oscillations of the building have decayed and there is no evidence of any permanent static displacement of the building. The full assessment of the static offset is complicated by the large thermal deformations of the building that we are still assessing. There is a finite element model of the building and it should be possible to compute the response of all floors of the tower to the ground motions. This detailed analysis, including determination of the Q of the building is in progress.

DATA AND RESOURCES

Sources of data:
IGS GPS site location information.
http://www.igs.org/igsnetwork/network_by_site.php?site=bshm
other site= values are nico, ista and kit3.
Data downloaded from:

ftp://cddis.gsfc.nasa.gov/gps/data/highrate/2017/<doy>/17d/18/ where doy is day of year. 18 is 18:00 GPS time and the bshm files are in 4 minutes pieces which were re-combined in to a single 1-hr file.

Images for Figure 2 were obtained and modified from http://www.som.com/projects/al_hamra_tower. Line drawings downloaded from https://images.adsttc.com/media/images/55e8/9e35/46fe/9f47/e100/00e8/slideshow/al-hamra-firdous-tower-14.jpg?1441308208. For details of the tower see . http://www.alhamra.com.kw/business-tower/facts-figuress/, Last accessed August 21, 2018.

Earthquake data used in this study were obtained from Kuwait the KNSN. The KNSN data are available upon request with approval from the Kuwait Institute for Scientific Research.

Seismic data from Malkishua, Israel (MMHI) is part of the Israel seismic network operated by the Geophysical Institute of Israel (http://seis.gii.co.il/en/network/seismicNetwork.php). Data were downloaded through IRIS data services https://ds.iris.edu/wilber3/find_stations/10485707 with network code IS used. Links last accessed August 21, 2018.

ACKNOWLEDGEMENTS

This project was sponsored by the Kuwait Foundation for the Advancement of Sciences. The project was conducted as part of the Kuwait-Massachusetts Institute of Technology signature project on sustainability of Kuwait's built environment under the direction of O. Büyüköztürk. The authors would like to thank Brendan Crowell, Yehuda Bock and an anonymous reviewer for useful comments that improved this paper. Part of this research was supported by NASA grant NNX09AK68G. Some of the figures were created by using the Generic Mapping Tools (Wessel et al., 2013) and MATLAB™.

References

Abdel-Fattah, R., A. Alenezi, F. Al-Jeri, and S. Abdul-Salam (2013) Assessment of seismic effects of selected sites in Kuwait city, *Final project report, KISR, EC081C*.

Agnew, D. C., and K. M. Larson (2007), Finding the repeat times of the GPS constellation, GPS Solutions, 11,71–76

Al-Qazweeni, J., H. Kamal, A. Al-Enezi, J. Parol, A. Abdulsalam, A. B. Nakhi, H. Sun (2018), Modeling, Data analysis and Structural Seismic Reliability of Tall Buildings, in *Sustainability of Kuwait's Built Environment*, O. Büyüköztürk, H. Kamal and M.N. Toksöz (Editors), 155-171.

Al-Sulaimi, J, and A Mukhopadhyay (2000). An Overview of the Surface and Near-Surface Geology, Geomorphology and Natural Resources of Kuwait. *Earth-Science Reviews* 50 (3–4). Elsevier: 227–67. doi:10.1016/S0012-8252(00)00005-2.

Bilich, Andria, and Kristine M. Larson. (2007). "Mapping the GPS Multipath Environment Using the Signal-to-Noise Ratio (SNR)." *Radio Science* 42 (6). doi:10.1029/2007RS003652.

Bock, Y., and D. Melgar. (2016). "Physical Applications of GPS Geodesy: A Review." *Reports on Progress in Physics* 79 (10). doi:10.1088/0034-4885/79/10/106801.

Çelebi, M., and H.-P. Liu (1998). Before and after retrofit–response of a building during ambient and strong motions. *J. Wind Eng. Ind. Aerodyn.*, 204 77, 259–268.

Çelebi, M., M. N. Toksöz, and O. Büyüköztürk (2014). Rocking behavior of an instrumented unique building on the MIT campus identified from ambient shaking data. *Earthq. Spectra*, 30(2), 705–720.

Choi, Kyuhong, A. Bilich, K. M. Larson, and P. Axelrad. (2004). "Modified Sidereal Filtering: Implications for High-Rate GPS Positioning." *Geophy. Res. Lett.* 31 (22): 1–4. doi:10.1029/2004GL021621.

Cleveland, W. S., and S. J. Devlin. (1988). Locally Weighted Regression: An Approach to Regression Analysis by Local Fitting. *Journal of the American Statistical Association* 83 (403): 596–610. doi:10.1080/01621459.1988.10478639.

Coccia, M. (2017). Processing strategies optimization and error mitigation of geodetic measurements (Doctoral dissertation, Massachusetts Institute of Technology). http://hdl.handle.net/1721.1/112431

Dow, J.M., R.E. Neilan, and C. Rizos (2009). The International GNSS Service in a changing landscape of Global Navigation Satellite Systems, *J. Geodesy* 83:191–198, DOI: 10.1007/s00190-008-0300-3 https://kb.igs.org/hc/en-us/article_attachments/200699673/s00190-008-0300-3.pdf

Genrich, J. F. and Y. Bock (2006), Instantaneous geodetic positioning with 10-50 Hz GPS Measurements: Noise characteristics and implications for monitoring networks*, J. Geophys. Res., 111, B03403,* doi:10.1029/2005JB003617.

Genrich, J. F. and Y. Bock (1992), Rapid resolution of crustal motion at short ranges with the Global Positioning System, *J. Geophys. Res., 97*, 3261-3269.

Gu, C., F. Al-Jeri, A. Al-Enezi, O. Büyüköztürk, & M.N. Toksöz (2017). Source Mechanism Study of Local Earthquakes in Kuwait. *Seismol. Res. Lett.*, 88(6), 1465-1471.

Gu, C., G.A. Prieto, A. Al-Enezi, F. Al-Jeri, J. Al-Qazweeni, H. Kamal, S. Kuleli, A. Mordret, O. Büyüköztürk, M.N. Toksöz (2018) Ground Motion in Kuwait from Regional and Local Earthquakes: Potential Effects on Tall Buildings, *Pure and Applied Geophysics*, doi: 10.1007/s00024-018-1943-5

Helffrich, G., J. Wookey, I. Bastow (2013) The Seismic Analysis Code: A Primer and User's Guide, *Cambridge University Press*, Computers, pp 173.

Havskov, J., and L. Ottemoller (1999) SeisAn Earthquake Analysis Software. *Seismological Research Letters* 70 (5). GeoScienceWorld: 532–34. doi:10.1785/gssrl.70.5.532.

Herring, T.A., R. W. King, and M. A. Floyd (2017), Introduction to GAMIT/GLOBK: Release 10.61, Massachusetts. Institute. of Technology, Cambridge.

Herring, T.A., M. Coccia, J. Parol, A. Al-Enezi, G. Al-Jeri, J. Al-Qazweeni, K. Hasan (2018), Global Position Systems for Building Deformation Monitoring, in *Sustainability of Kuwait's Built Environment*, O. Büyüköztürk, H. Kamal and M.N. Toksöz (Editors), 117-131.

Kohler, M. D., P. M. Davis, and E. Safak (2005), Earthquake and ambient vibration monitoring of the steel-frame ucla factor building, *Earthq. Spec.*, 21(3), 715–736.

Mordret, A., H. Sun, G.A. Prieto, M.N. Toksöz, , & O. Büyüköztürk (2017). Continuous Monitoring of High-Rise Buildings Using Seismic Interferometry. *Bull. Seismol. Soc. Am.*, 107(6), 2759-2773.

Prieto, G. A., J. F. Lawrence, A. I. Chung, and M. D. Kohler (2010), Impulse response of civil structures from ambient noise analysis, *Bull. Seismol. Soc. Am.*, 100(5A), 2322–2328.

Saunders, J. K., D. E. Goldberg, J. S. Haase, Y. Bock, D. G. Offield, D. Melgar, J. Restrepo, R. B. Fleischman, A. Nema, J. Geng, C. Walls, D. Mann, G. Mattioli (2016), Seismogeodesy using GNSS and low-cost MEMS accelerometers: perspectives for earthquake early warning and rapid response, *Bull. Seismol. Soc. Am., 106*, 6, 2469–2489, doi: 10.1785/0120160062.

Shakal, A. F., M. J. Huang, and R. B. Darragh (1996). Interpretation of significant ground-response and structure strong motions recorded during the 1994 Northridge earthquake. *Bull. Seismol. Soc. Am.*, 86(1B), S231-S246.

Snieder, R., and E. Sáfak (2006), Extracting the building response using seismic interferometry: Theory and application to the millikan library in pasadena, california, *Bull. Seismol. Soc. Am.*, 96(2), 586–598.

Sun, H., A. Mordret, G.A. Prieto, M.N. Toksöz, and O. Büyüköztürk (2017), Bayesian characterization of buildings using seismic interferometry on ambient vibrations. *Mech. Sys. Sig. Proc.*, 85, 468-486.

Sun, H., O. Büyüköztürk (2018), Computational Modeling of Al-Hamra Tower for Structural Health Monitoring, in *Sustainability of Kuwait's Built Environment*, O. Büyüköztürk, H. Kamal and M.N. Toksöz (Editors), 132-141.

Toksöz, M.N., C. Gu, S. Kuleli, O. Büyüköztürk, A. Al-Enezi, F. Al-Jeri, H. Kamal (2018), Ground motion modeling, in *Sustainability of Kuwait's Built Environment*, O. Büyüköztürk, H. Kamal and M.N. Toksöz (Editors), 101-116.

U.S. Geological Survey [USGS] (2017) M 7.3 - 29km S of Halabjah, Iraq, https://earthquake.usgs.gov/earthquakes/eventpage/us2000bmcg#executive, (last accessed August, 2018)

Wessel, P., W. H. F. Smith, R. Scharroo, J. F. Luis, and F. Wobbe (2013), Generic Mapping Tools: Improved version released, *Eos Trans. AGU*, *94*, 409–410, doi:10.1002/2013EO450001.

List of figure captions

Figure 1. The photograph of Al-Hamra Tower, Kuwait City, Kuwait. (For details about the building see data resources link)

Figure 2. Map of earthquake and of main GPS and seismic stations used in this paper. (a) The 12 Nov 2017 Mw 7.3 earthquake and GPS and broad-band seismic stations in a geographic map. The blue star shows the hypocenter of the earthquake, the blue beach ball shows the source mechanism, the yellow circle is the Kuwait City, the red rectangle is region that Kuwait National Seismic Network (KNSN) covers, the white diamond shows GPS station BSHM in Israel, the white triangles show station RAYN in Saudi Arabia and station UOSS in UAE. This earthquake was widely felt in Kuwait. (b) The two GPS stations (red diamonds) – KISP at the roof of a 2-story building at the Kuwait Institute for Scientific Research (KISR) and ALHR on the top of the Al-Hamra Tower – and eight stations of KNSN throughout Kuwait (green triangles). (c) The ground displacements calculated from the seismograms at KB site (red lines). (d) The measured displacements from GPS station KISP w.r.t. BSHM (black lines). The blue and green lines are GPS measured displacements of KISP w.r.t. BSHM on the day before and after the earthquake, processed in the same way as the GPS data due to the earthquake. The RMS scatter of the non-earthquake traces, shown as error bars at the start of data, are 2.3, 2.0, and 4.3 mm in the North, East and Up directions.

Figure 3. Location of the GPS antenna at the 86th floor of the Al-Hamra building viewed from the south east (a) and close to east as a line drawing (b). Insert (c) shows the GPS antenna mounted about half a meter about the curtain wall. The sky view from the 86th floor site, ALHR, is only partly obstructed by the building. There is also a site located on the Mall roof site, MLRF, which is obstructed by this and other buildings in the area.

Figure 4. The comparison of measured displacements from GPS station KISP w.r.t. BSHM (black lines) and seismic station KB (red lines). The origin time of KB has been offset by 2.5 seconds to account for the different distance to the epicenter. The blue and green lines, offset for clarity, are GPS measured displacements of KISP w.r.t. BSHM on the day before and after the earthquake, processed in the same way as the GPS data due to the earthquake. The RMS scatter of the non-earthquake traces, shown as error bars at the start of data, are 2.3, 2.0, and 4.3 mm in the North, East and Up directions.

Figure 5. The comparison of measured displacements from GPS station ALHR w.r.t. BSHM (black lines) and seismic station KB (red lines). The blue and green lines, offset for clarity, are GPS measured displacements of ALHR w.r.t. BSHM on the day before and after the earthquake, processed in the same way as the GPS data due to the earthquake. The RMS are 2.1, 2.8, and 4.7 mm in the North, East and Up directions.

Figure 6. (a) Amplitude spectra, calculated using ambient noise data recorded by one Kinemetrics EpiSensor instrument, at the 80^{th} floor of the Al-Hamra Tower. Average spectra for data collected on November 25, 2014, were computed with a 600 s moving window. (b) The GPS measured north and east displacements from station ALHR w.r.t. KISP (black lines). The blue and green lines, offset for clarity, are GPS measured displacements of ALHR w.r.t. KISP on the day before and after the earthquake, processed in the same way as the GPS data due to the earthquake. The RMS scatter of the non-earthquake traces, shown as error bars at the start of data, are 2.0, 3.0 in the north and east directions.

Figure 7. The black line shows the horizontal moving window average amplitude of ALHR w.r.t. KISP filtered between 120 and 180 mHz (periods 8.3-5.6 seconds). The red (KB site) and blue (KISP GPS site) show the same type of analysis with the amplitudes multiplied by 10. All amplitudes are smoothed by a 10 sec moving average window.

Full mailing address for each author
Thomas Herring, 54-322, Massachusetts Institute of Technology, 77 Massachusetts Avenue, Cambridge, MA 02139 USA

Chen Gu, 54-617, Massachusetts Institute of Technology, 77 Massachusetts Avenue, Cambridge, MA 02139 USA

M. Nafi Toksöz, 54-614, Massachusetts Institute of Technology, 77 Massachusetts Avenue, Cambridge, MA 02139 USA

Oral Büyüköztürk, 1-281, Massachusetts Institute of Technology, 77 Massachusetts Avenue, Cambridge, MA 02139 USA

Jafarali Parol, Abdullah Al-Enezi, Farah Al-Jeri, Jamal Al-Qazweeni, Hasan Kamal, Kuwait Institute for Scientific Research, Kuwait City, 13109, Kuwait

Tables

Table 1: Locations of GPS and seismic sites

Description	Code	Latitude (deg)	Longitude (deg)	Ellipsoidal Height (m)
Mw 7.3 Iran/Iraq Earthquake		34.905	45.956	-19 km (depth)
Haifa, Israel	BSHM	32.779	35.023	225.073
KISR, Kuwait	KISP[1]	29.341	47.907	0.575
86th floor, Al-Hamra, Kuwait	ALHR[1]	29.379	47.993	388.248
Mall Roof, Al-Hamra, Kuwait	MLRF[1]	29.378	47.993	17.923
Kitab, Uzbekistan	KIT3	39.135	66.885	622.532
Nicosia, Greece	NICO	35.141	33.396	190.006
Istanbul, Turkey	ISTA	41.104	29.019	147.240
KB seismic station, Kuwait	KB	29.176	47.692	

[1]The GPS systems in Kuwait (ALHR, KISP, MLRF) use Trimble™ NetR9 receivers, tracking only GPS signals, with Trimble™ Zephyr GNSS Geodetic II (TRM57971.00) antennas.

Table 2: Distances and Azimuths between locations and sites in Table 1.

Location/Site	Site	Distance (km)	Azimuth (deg)
Earthquake Epicenter	KISP	643.86	162.86
Earthquake Epicenter	ALHR	642.13	162.03
Earthquake Epicenter	MLRF	642.26	162.04
Earthquake Epicenter	KB	656.06	165.06
Earthquake Epicenter	BSHM	1038.43	259.97
Earthquake Epicenter	KIT3	1915.94	69.66
Earthquake Epicenter	NICO	1145.76	274.92
Earthquake Epicenter	ISTA	1635.20	299.90
BSHM	KISP	1286.44	103.82

BSHM	ALHR	1292.78	103.51
KISP	ALHR	9.39	62.82
KISP	KB	27.78	228.96
KISP	KIT3	2051.93	53.02
KISP	NICO	1509.18	298.95
KISP	ISTA	2150.65	312.41
ALHR	MLRF	0.14	190.72
ALHR	KIT3	2042.68	53.02
ALHR	NICO	1514.43	298.70
ALHR	ISTA	2153.95	312.23

List of Figure captions

Figures:

Figure 1. The photograph of Al-Hamra Tower, Kuwait City, Kuwait. (For details about the building see data resources link)

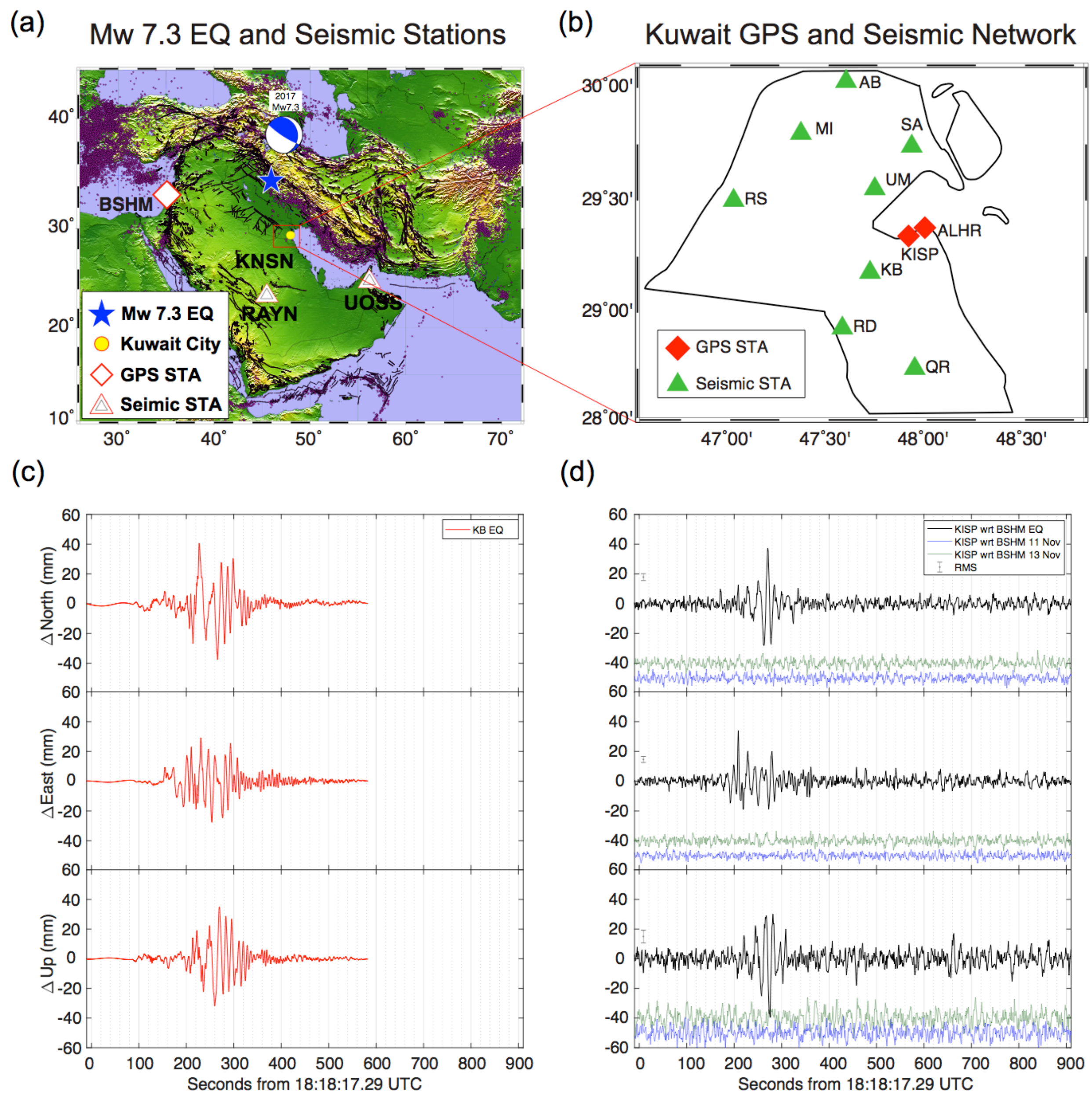

Figure 2. Map of earthquake and of main GPS and seismic stations used in this paper. (a) The 12 Nov 2017 Mw 7.3 earthquake and GPS and broad-band seismic stations in a geographic map. The blue star shows the hypocenter of the earthquake, the blue beach ball shows the source mechanism, the yellow circle is the Kuwait City, the red rectangle is region that Kuwait National Seismic Network (KNSN) covers, the white diamond shows GPS station BSHM in Israel, the white triangles show station RAYN in Saudi Arabia and station UOSS in UAE. This earthquake was widely felt in Kuwait. (b) The two GPS stations (red diamonds) – KISP at the roof of a 2-story building at the Kuwait Institute for Scientific Research (KISR) and ALHR on the top of the

Al-Hamra Tower – and eight stations of KNSN throughout Kuwait (green triangles). (c) The ground displacements calculated from the seismograms at KB site (red lines). (d) The measured displacements from GPS station KISP w.r.t. BSHM (black lines). The blue and green lines are GPS measured displacements of KISP w.r.t. BSHM on the day before and after the earthquake, processed in the same way as the GPS data due to the earthquake. The RMS scatter of the non-earthquake traces, shown as error bars at the start of data, are 2.3, 2.0, and 4.3 mm in the North, East and Up directions.

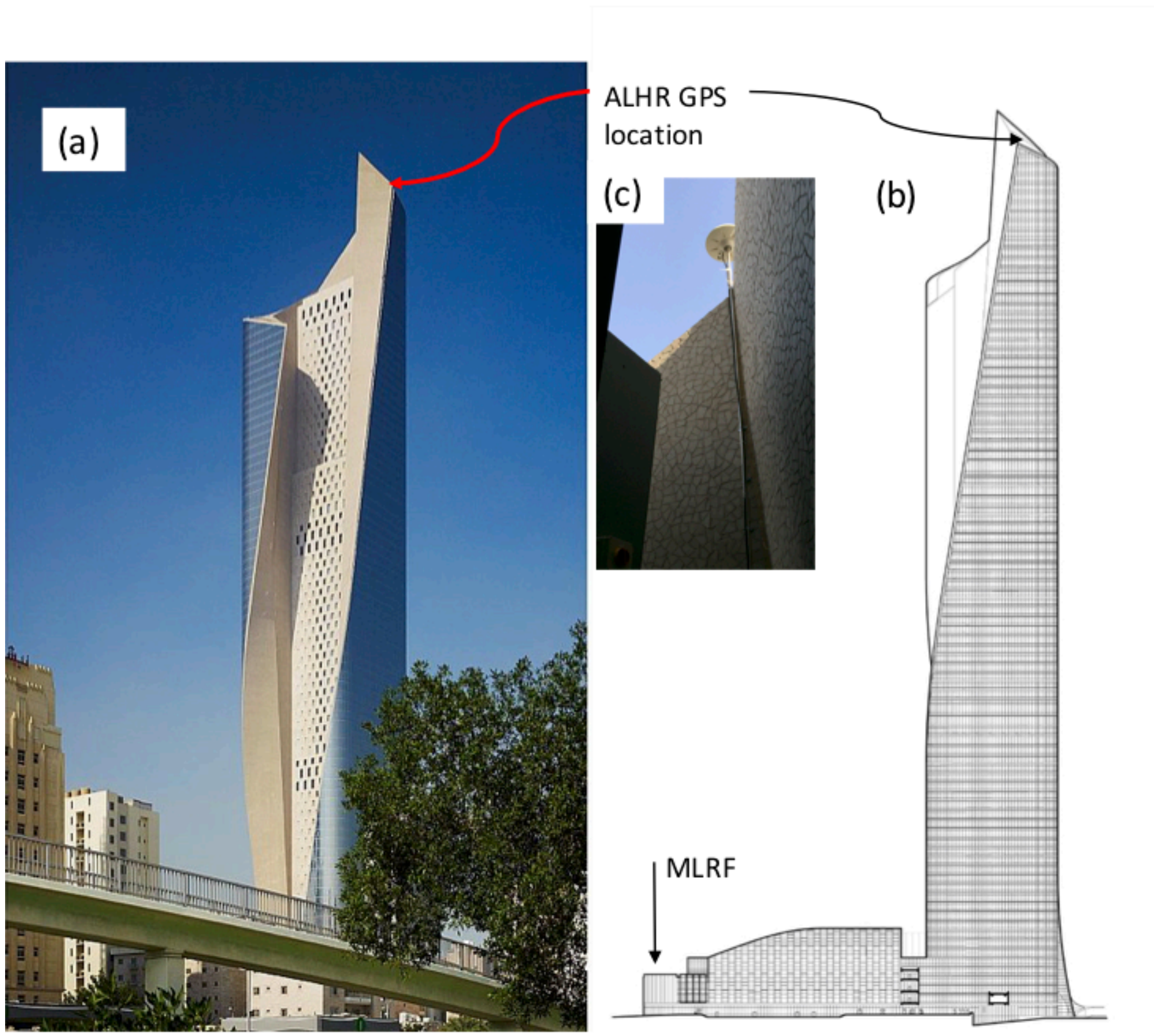

From http://www.som.com/projects/al_hamra_tower

Figure 3. Location of the GPS antenna at the 86th floor of the Al-Hamra building viewed from the south east (a) and close to east as a line drawing (b). Insert (c) shows the GPS antenna mounted about half a meter about the curtain wall. The sky view from the 86th floor site, ALHR, is only partly obstructed by the building. There is also a site located on the Mall roof site, MLRF, which is obstructed by this and other buildings in the area.

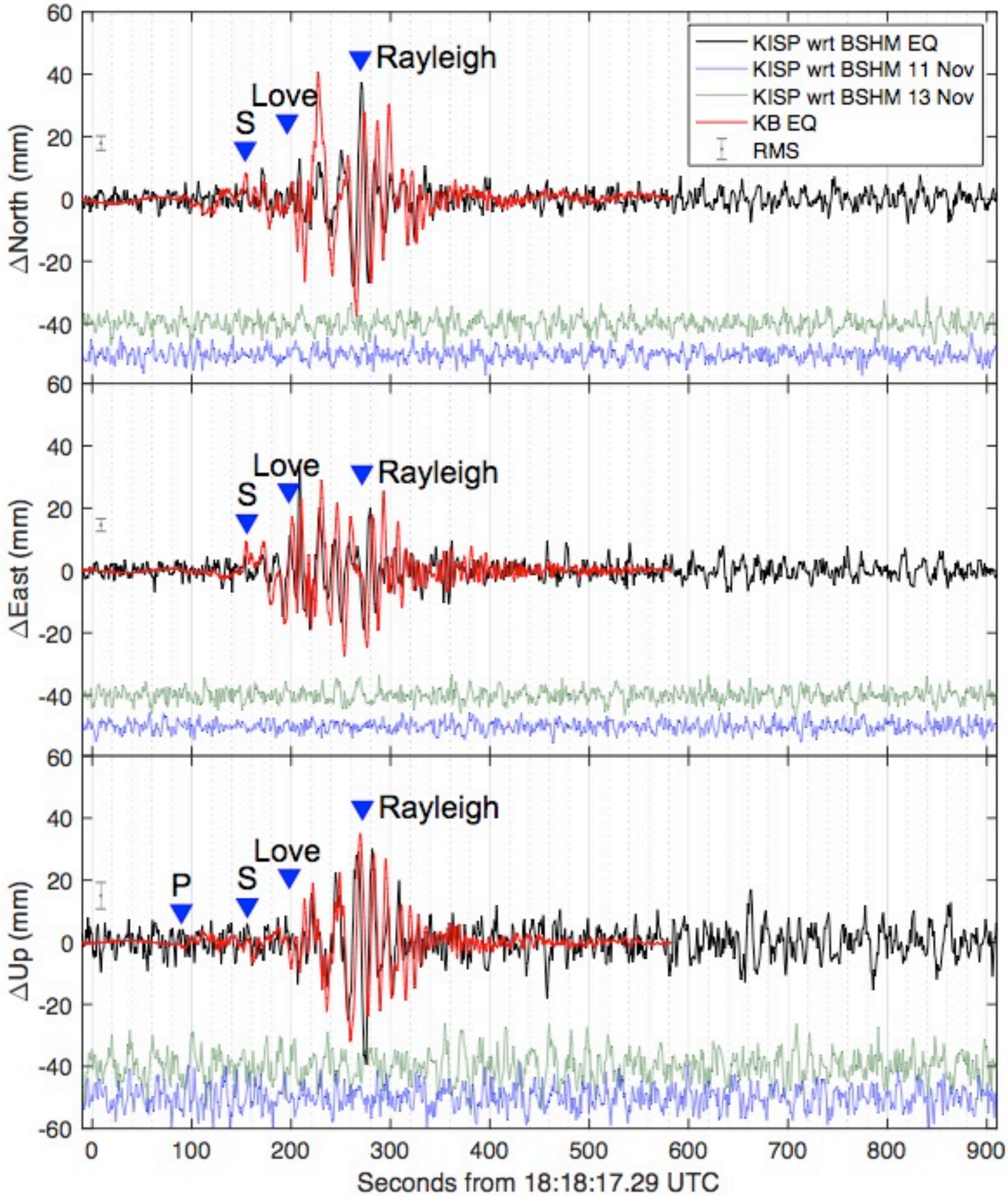

Figure 4. The comparison of measured displacements from GPS station KISP w.r.t. BSHM (black lines) and seismic station KB (red lines). The origin time of KB has been offset by 2.5 seconds to account for the different distance to the epicenter. The blue and green lines, offset for clarity, are GPS measured displacements of KISP w.r.t. BSHM on the day before and after the earthquake, processed in the same way as the GPS data due to the earthquake. The RMS scatter

of the non-earthquake traces, shown as error bars at the start of data, are 2.3, 2.0, and 4.3 mm in the North, East and Up directions.

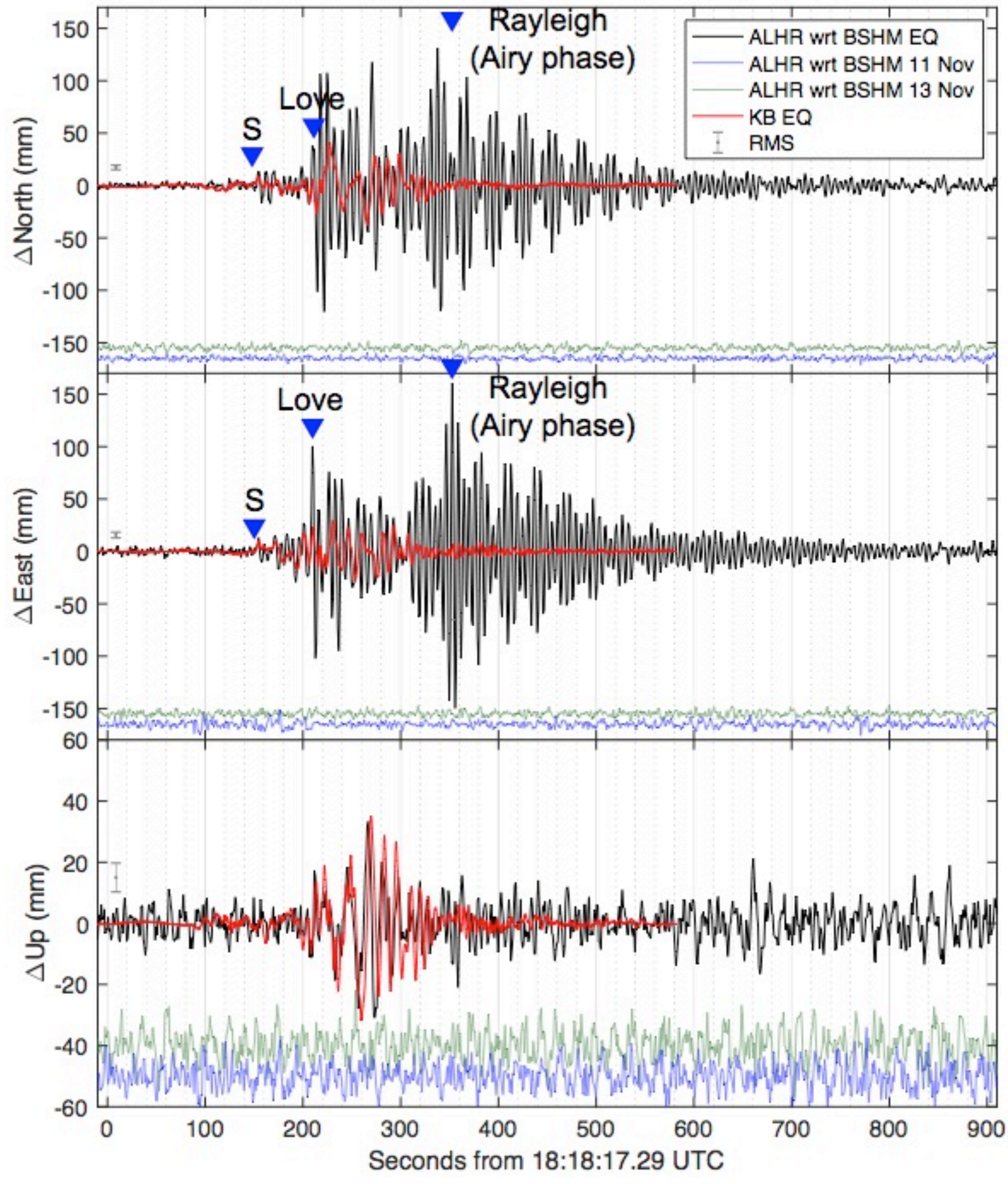

Figure 5. The comparison of measured displacements from GPS station ALHR w.r.t. BSHM (black lines) and seismic station KB (red lines). The blue and green lines, offset for clarity, are GPS measured displacements of ALHR w.r.t. BSHM on the day before and after the earthquake, processed in the same way as the GPS data due to the earthquake. The RMS are 2.1, 2.8, and 4.7 mm in the North, East and Up directions.

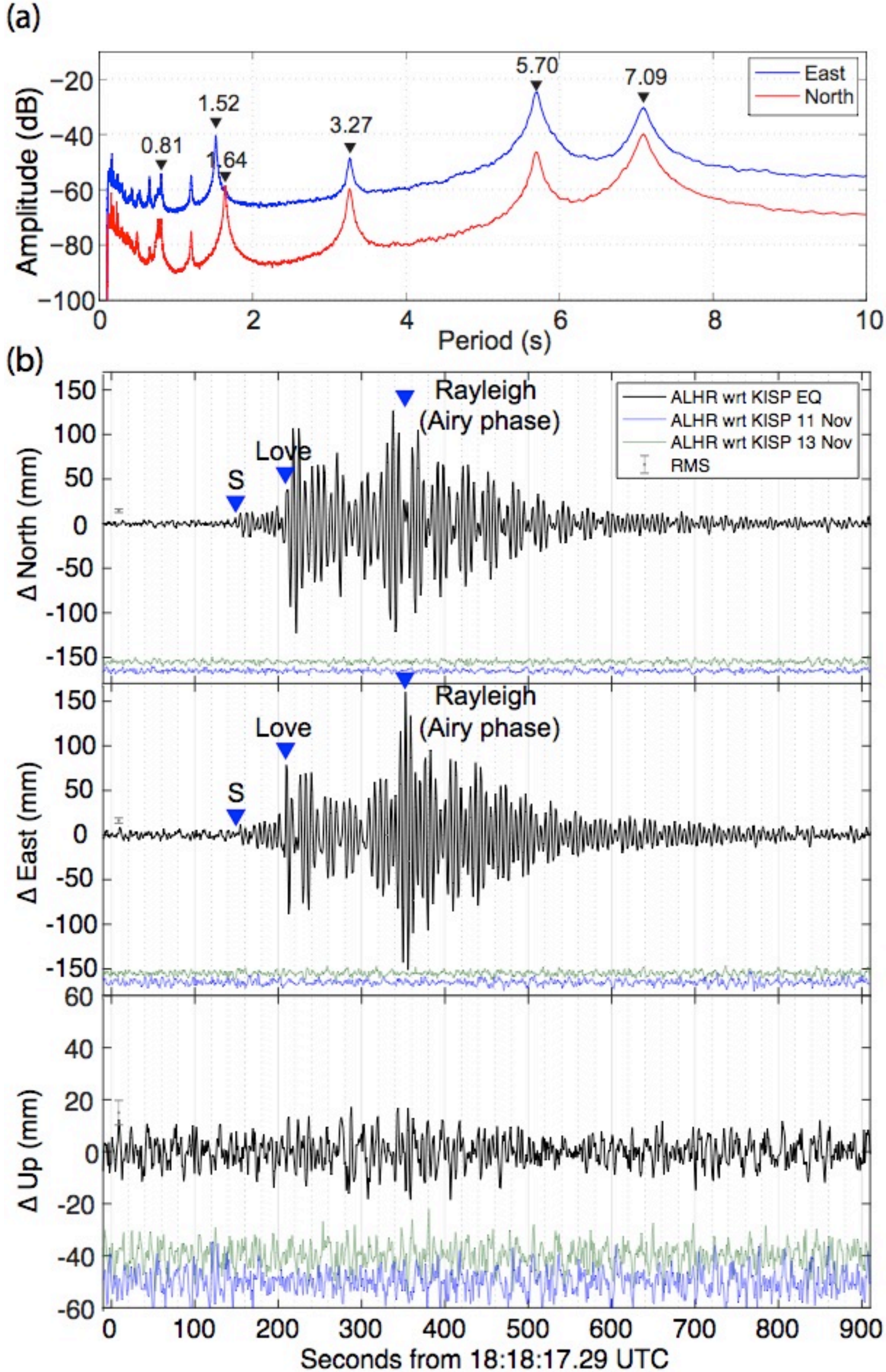
(a)
Amplitude (dB)
Period (s)
East
North
0.81
1.52
1.64
3.27
5.70
7.09
(b)
Δ North (mm)
Δ East (mm)
Δ Up (mm)
S
Love
Rayleigh
(Airy phase)
ALHR wrt KISP EQ
ALHR wrt KISP 11 Nov
ALHR wrt KISP 13 Nov
RMS
Seconds from 18:18:17.29 UTC

Figure 6. (a) Amplitude spectra, calculated using ambient noise data recorded by one Kinematics EpiSensor instrument, at the 80^{th} floor of the Al-Hamra Tower. Average spectra for data collected on November 25, 2014, were computed with a 600 s moving window. (b) The GPS measured north and east displacements from station ALHR w.r.t. KISP (black lines). The blue and green lines, offset for clarity, are GPS measured displacements of ALHR w.r.t. KISP on the day before and after the earthquake, processed in the same way as the GPS data due to the earthquake. The RMS scatter of the non-earthquake traces, shown as error bars at the start of data, are 2.0, 3.0 in the north and east directions.

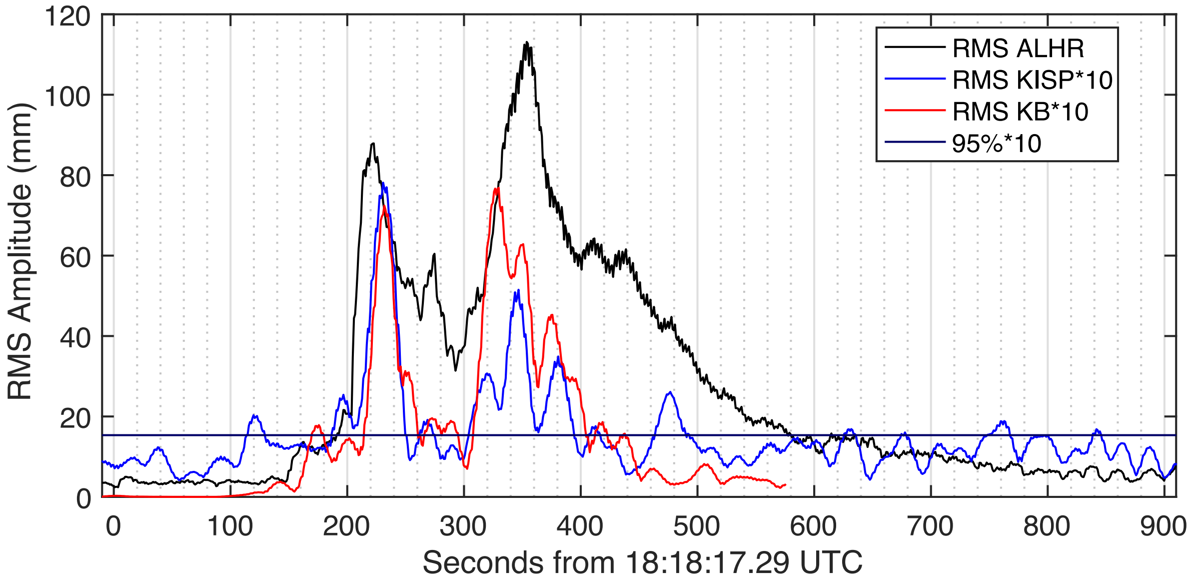

Figure 7. The black line shows the horizontal moving window average amplitude of ALHR w.r.t. KISP filtered between 120 and 180 mHz (periods 8.3-5.6 seconds). The red (KB site) and blue (KISP GPS site) show the same type of analysis with the amplitudes multiplied by 10. All amplitudes are smoothed by a 10 sec moving average window.